HIGH-ALTITUDE AIR MASS ZERO CALIBRATION OF SOLAR CELLS[1]

James R. Woodyard
Wayne State University, Detroit, Michigan

David B. Snyder, NASA Glenn Research Center
Cleveland, Ohio

ABSTRACT

Air mass zero calibration of solar cells has been carried out for several years by NASA Glenn Research Center using a Lear-25 aircraft and Langley plots. The calibration flights are carried out during early fall and late winter when the tropopause is at the lowest altitude. Measurements are made starting at about 50,000 feet and continue down to the tropopause. A joint NASA/Wayne State University program called Suntracker is underway to explore the use of weather balloon and communication technologies to characterize solar cells at elevations up to about 100 kft. The balloon flights are low-cost and can be carried out any time of the year. AM0 solar cell characterization employing the mountaintop, aircraft and balloon methods are reviewed. Results of cell characterization with the Suntracker are reported and compared with the NASA Glenn Research Center aircraft method.

INTRODUCTION

It is important in characterizing solar cells for use in space-power applications that the spectral irradiance of the calibration-light source is within a percent of the spectral irradiance of air mass zero conditions (AM0). Spectral irradiance differences greater than a few percent can result in calibration errors; the magnitude of the errors depends on the structure of the solar cell. In the case of single-junction cells, the current-voltage characteristics are not very sensitive to small differences in the spectral irradiances of calibration-light sources because the spectral response is not sensitive to spectral irradiance. The current in a single-junction solar cell under AM0 normal incidence operating at a voltage V is given by

$$I_o(V) = \int_{\lambda 1}^{\lambda 2} S_o(\lambda) R(\lambda, V) d\lambda \tag{1}$$

where $S_o(\lambda)$ is the absolute AM0 spectral irradiance of sunlight and $R(\lambda, V)$ is the spectral response of the cell at wavelength λ and voltage V. In the ideal case, the spectral response is independent of the irradiance of the light source. The spectral response depends on the opto-electronic properties of the materials used in the fabrication of the cell that include, but are not limited to, the wavelength dependence of the optical absorption coefficient; optical band gap, material thickness, doping, temperature and quality; and carrier mobility and lifetime. $\lambda 1$ and $\lambda 2$ are the lower and upper cut-off wavelength values where the spectral response no longer contributes to cell current.

The spectral irradiance of laboratory-based solar simulators is different than the AM0 spectral irradiance. The simulator is set to “AM0” intensity by adjusting the intensity to produce the short-circuit current in a standard cell,

[1] This work was supported in part under NASA Grant NAG3-2801.

i.e., a cell calibrated under AM0 conditions. This approach may be used because the spectral response of single-junction solar cells is somewhat insensitive to spectral irradiance. Adjusting the intensity of the simulator will compensate for spectral irradiance differences when compared to AM0 over the range of the spectral response of the cell. The adjustment produces a spectral irradiance that is larger than AM0 in some regions of the spectrum and smaller than AM0 in other regions of the spectrum. Following adjustment of the simulator intensity, cells may be characterized under "AM0" conditions. This method may be used as long as two conditions are met. First, it is necessary that the simulator is stable, meaning that spectral irradiance remains constant during the measurements on the standard cell and the cells to be characterized. Second, the voltage dependence of the spectral responses of the standard cell and cells to be characterized must be the same and not influenced by differences in the spectral irradiances of the solar simulator and AM0. The method requires stable standard cells for each of the types of single-junction cells to be characterized. Laboratory-based "AM0"characterization of single-junction solar cells has been carried out for many years with good results using this method.

The evolution of solar-cell technology for space applications has resulted in "state-of-the-art" cells with four and five junctions in series. Each junction is designed with a spectral response matched to one region of the spectral irradiance of AM0 in order to optimize the efficiency of solar cells. The current in a four-junction solar cell operating at a given voltage is given by:

$$I_o(V) = \int_{\lambda 1}^{\lambda 8} S_o(\lambda) R(\lambda, V) d\lambda \text{ and} \tag{2}$$

$$I_o(V) = \int_{\lambda 1}^{\lambda 2} S_o(\lambda) R_1(\lambda, V_1) d\lambda = \int_{\lambda 3}^{\lambda 4} S_o(\lambda) R_2(\lambda, V_2) d\lambda = \int_{\lambda 5}^{\lambda 6} S_o(\lambda) R_3(\lambda, V_3) d\lambda = \int_{\lambda 7}^{\lambda 8} S_o(\lambda) R_4(\lambda, V_4) d\lambda \tag{3}$$

where the variables in Equation 2 are the same as in Equation 1 except $\lambda 1$ and $\lambda 8$ are the lower and upper cut-off wavelength values, above and below which the spectral response is negligible and no longer contributes to cell current. The spectral response in Equation 2 characterizes the overall operation of the four junctions in optical absorption and carrier transport. However, the spectral responses and voltages in Equation 3, $R_i(\lambda, V_i)$ and V_i respectively, are subscripted to show that they are different for each of the four junctions. The voltage across the cell is equal to the sum of the voltages across each of the four junctions, namely, $V = \sum_{i=1}^{i=4} V_i$. The wavelength ranges on each of the integrals, in the most general case, will overlap since it is not possible to fabricate materials with sharp wavelength cut-offs. Equation 3 shows the series nature of the current in multi-junction solar cells, namely, the current is the same in each of the junctions.

The sensitivity of a four-junction solar cell to spectral irradiance can be illustrated with an example. Consider a cell that has been optimally designed for AM0 is to be characterized with a solar simulator. Assume the solar simulator has a spectral irradiance that is less than AM0 in the $\lambda 1$ and $\lambda 2$ wavelength range and the same as AM0 in the other three wavelength ranges shown in Equation 3. The lower spectral irradiance will result in less current in the junction optimized for the $\lambda 1$ and $\lambda 2$ wavelength range which in turn will limit the current in the cell due to the series nature of the four junctions. Equation 3 shows that the current reduction in the four junctions must be accomplished through changes in spectral responses of the other three junctions; this is the case because the spectral irradiances in the other three wavelength ranges are assumed to be the same as AM0. The collective interaction of the four junctions will result in redistribution of the cell voltage across the four junctions, which in turn changes the spectral responses of the four junctions and the cell current.

The role of the interaction of four junctions in the operation of a multi-junction solar cell, as compared to a single-junction cell, can be illustrated with an example. Assume the average spectral irradiance and the average spectral response are the same in the four wavelength regions in Equation 3. A one percent decrease in the spectral irradiance relative to AM0 over the $\lambda 1$ and $\lambda 2$ wavelength range will result in about a one percent decrease in the cell short-circuit current. A single-junction junction solar cell that responds in a similar fashion

over the $\lambda 1$ to $\lambda 8$ wavelength range will experience only a 0.25 % decrease in short-circuit current. The reason is a one percent decrease in the integrated spectral irradiance over the $\lambda 1$ and $\lambda 2$ wavelength range in the multi-junction cell corresponds to a 0.25 % decrease in the integrated spectral irradiance over the $\lambda 1$ to $\lambda 8$ wavelength range in the single-junction cell

A calibration procedure for multi-junction solar cells that uses a standard cell to set a solar simulator to "AM0" intensity may result in data that are not useful in optimizing the design of a test cell for space power generation. Assuming the voltage dependence of the spectral responses of each of the junctions in the standard and test cells are the same under the simulator "AM0" conditions, the junctions may be operating under conditions that are vastly different than AM0 conditions. It is possible that the test cell current-voltage characteristics measured under "AM0" conditions may not be useful in optimizing the cell design to improve efficiencies at the one percent level. Moreover, the complex nature of the interaction of the junctions does not lend itself to the use of an optical technique to compensate for the deficiencies in the "AM0" spectral irradiance.

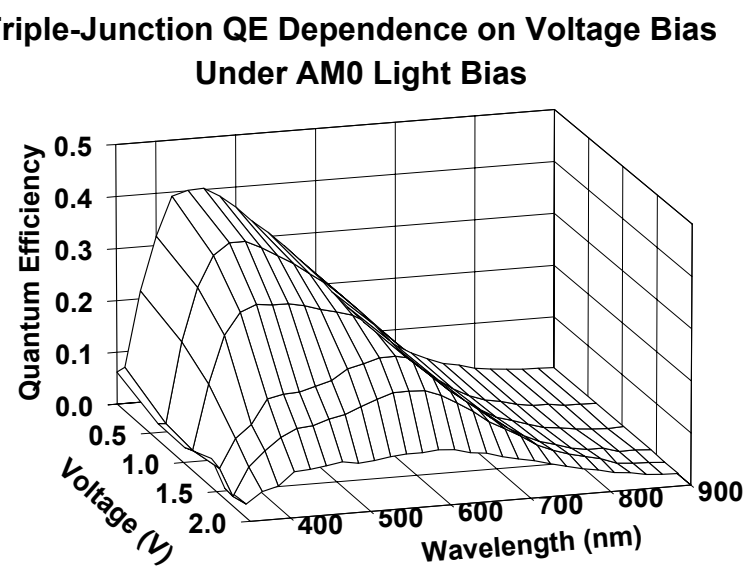

Figure 1. Dependence of quantum efficiency of an a-Si:H alloy-based triple-junction thin-film solar cell on forward bias [1]

The differences in the "AM0" and AM0 spectral irradiances are more problematic at the maximum power point than short-circuit conditions. The reason is the electrostatic potential barriers in each of the junctions are relatively small at the maximum power point as compared to short-circuit current conditions. Redistribution of voltages across the junctions can produce relatively large changes in the electrostatic potential barriers and produce major changes in the spectral responses of the junctions. Figure 1 shows the effect of forward bias on the quantum efficiency of a solar cell [1]. The solar cell is a triple-junction a-Si:H alloy-based thin-film solar cell that was illuminated with a solar simulator with an AM0 spectral irradiance. The spectral irradiance was within one percent of AM0 in the wavelength range where the spectral response contributed to cell current. The figure shows the maximum quantum efficiency is at a wavelength of about 450 nm, serving as evidence that the top junction in this particular cell was limiting the current of the cell under short-circuit conditions. The maximum in the quantum efficiency shifted from 450 to 600 nm as the forward bias approached the maximum-power point showing that the middle and bottom junctions limited the cell current. The quantum efficiency of the cell changed markedly when the spectral irradiance of the simulator was altered [1]. A history of particle irradiation can also have a large effect on the dependence of the quantum efficiency of multi-junction cells on forward bias thereby further complicating the optimization of design of cells for space power generation in radiation environments.

It is clear that the voltage dependence of the spectral responses of multi-junction solar cells complicates optimization of cell design. While there are characterization methods that make it possible to use solar simulators in advancing the multi-junction solar cell technology, the series nature of the cells places more demands on the need for standard cells characterized under AM0 conditions. AM0 conditions are available only in space; near AM0 conditions can be achieved at altitudes in excess of 100,000 ft. The demand for greater access to AM0, and the costs associated with AM0 calibration, has generated interest in exploring lost-cost methods for AM0 solar cell calibration. The NASA supported Suntracker program is an attempt to meet this challenge.

AM0 SOLAR CELL CALIBRATION MEHTODS

Efforts to develop new methods for AM0 calibration of solar cells should be founded in an awareness of current calibration methods, a knowledge of fundamental principles, and possible shortcomings of existing methods. Reviewing analyses of data collected by various methods is also an instructive way to gain a better understanding of the methods. Mountaintop, aircraft and balloon-based methods for AM0 calibration of solar cells are reported in the literature. While there have been a number of satellite-based measurements, no space calibration method has emerged that is available to the photovoltaic community for producing solar cell standards. A photovoltaic engineering test bed facility for use on the International Space Station has been designed but not implemented [2]. This section will review the mountaintop, aircraft and balloon-based methods used in AM0 calibration of solar cells.

Mountaintop method

Laboratory-based solar simulators have been used since solar cells became attractive for space-power applications. However, it was recognized by Zoutendyk that sunlight should be used " to diminish uncertainty in the design of space solar cell power systems" [3]. He was one of the first investigators to attempt to correct for the effects of the atmosphere on the spectral irradiance of sunlight. A review of his work with silicon single-junction solar cells serves as a basis for understanding some of the challenges associated with AM0 calibration methods.

Zoutendyk assumed the spectral irradiance at a given air mass $S_m(\lambda)$ is given by:

$$S_m(\lambda) = S_o(\lambda)e^{-\alpha(\lambda)m} \tag{4}$$

where $\alpha(\lambda)$ is the monochromatic atmospheric absorption coefficient per unit air mass and m is the geometric air mass. He defined the geometric air mass as the ratio of the path length of the sunlight through the atmosphere at a zenith angle θ to the path length for the sunlight when the sun is overhead and the zenith angle is zero. The geometric air mass was taken as the secant of the zenith angle, namely, $m = \sec(\theta)$. The sea-level irradiance at a given air mass is:

$$S_m = \int_{\circ}^{\infty} S_o(\lambda)e^{-\alpha(\lambda)m}d\lambda \,. \tag{5}$$

The monochromatic short-circuit current at a given air mass was assumed to be given by:

$$I_{scm}(\lambda) = I_{sc0}(\lambda)e^{-\alpha(\lambda)m} \quad \text{where} \quad I_{sco}(\lambda) = R(\lambda)S_o(\lambda) \tag{6}$$

where $I_{sco}(\lambda)$ is the monochromatic short-circuit current under AM0 conditions. The short-circuit current of a single-junction cell over $\lambda 1$ to $\lambda 2$ wavelength range where the spectral response contributes to the current is:

$$I_{scm} = \int_{\lambda 1}^{\lambda 2} R(\lambda)S_o(\lambda)e^{-\alpha(\lambda)m}d\lambda = \int_{\lambda 2}^{\lambda 2} I_{sc0}(\lambda)e^{-\alpha(\lambda)m}d\lambda \,. \tag{7}$$

Equation 7 serves as the basis for the use of Langley plots to characterize solar cells. The exponential term may be factored out of the integral if $\alpha(\lambda)$ is assumed to be constant over the $\lambda 1$ and $\lambda 2$ wavelength range. The short-circuit current for a given air mass can then be written as:

$$I_{scm} = e^{-\alpha m} \int_{\lambda 1}^{\lambda 2} I_{sco}(\lambda) d\lambda = e^{-\alpha m} I_{sco} \tag{8}$$

where I_{sco} is the AM0 cell short-circuit current. Taking the Log_{10} of both sides of Equation 8 gives:

$$Log_{10} I_{scm} = -0.4343 \alpha m + Log_{10} I_{sco} \tag{9}$$

which is the theoretical equation used to determine the short-circuit current of solar cells under AM0 conditions. The logarithm of the short-circuit current is plotted on the ordinate of a semi-log graph and the air mass on the abscissa. The graph is referred to as a Langley plot. The data are fitted to a straight line using a least-squared method and the line extrapolated to $m = 0$. The intercept of the straight line with the ordinate is taken as the short-circuit current under AM0 conditions. The slope of the graph is -0.4343α and may be used to determine the atmospheric optical absorption coefficient. It is important to emphasize the constancy of the atmospheric optical absorption coefficient and the use of the "air mass" concept implies the following:

1. The optical absorption coefficient must be constant with respect to wavelength over the range of wavelengths where the solar cell spectral response contributes to cell current. If it is not constant, using Equation 9 to analyze data will produce errors in the extrapolated AM0 short-circuit current.

2. The concentration of optically absorbing atomic and molecular species in the atmosphere and their altitude dependence must not change for the duration of the short-circuit current as a function of air mass measurements. If the concentrations are changing during the measurements as a result of weather fronts, turbulence in the atmospheric, solar heating of the atmosphere etc., Equation 9 may not be linear and linear extrapolation of the short-circuit current to zero air mass may be in error.

3. The optical absorption coefficient must not be large enough to totally absorb the AM0 spectral irradiance at any air mass over the range of wavelengths where the solar cell spectral response contributes to cell current. If there are regions of the spectral irradiance where the sunlight is totally absorbed as it travels through the air mass, then the use of the Langley method to determine the AM0 short circuit will produce erroneous results.

4. Only normally incident sunlight must contribute to the short-circuit current. Scattered sunlight, referred to as "sky radiation" by Zoutendyk, must not contribute to the short-circuit current. Additionally, the presence of reflected light, or light produced by any other mechanisms, may introduce errors in the determination of the AM0 short-circuit current.

Zoutendyk set up a tracking system with silicon single-junction solar cells at an elevation of 7.4 kft on a mountaintop and carried out diurnal measurements of cell short-circuit current and temperature as a function of the zenith angle as the sun moved across the sky. The cell short-circuit current was defined at the current through a 1.000 Ω precision resistor in series with the cell. The sea level geometric air mass was calculated using $m = \sec(\theta)$. The data were analyzed using a Langley plot to arrive at cell AM0 short-circuit currents. The short-circuit current was corrected for cell temperature, precision resistor temperature and the earth-sun distance. The cells were then flown on the Ranger III spacecraft and cell data downlinked. The agreement between the AM0 short-circuit current measurements on the mountaintop and space was reported to be $\pm 2\%$ [3].

It is noteworthy to evaluate the constancy of the atmospheric optical absorption coefficient in mountaintop work to understand the utility of Langley plots. Equations 8 and 9 show that the exponential term is assumed to be constant over the $\lambda 1$ and $\lambda 2$ wavelength range in order to permit factoring it out of the integral. The cut off wavelength of Zoutendyk's solar cell at low wavelengths was $\lambda 1 = 450\ nm$ because of the optical properties of the cover glass on the cells. The high wavelength cut off was about $\lambda 2 = 1200\ nm$ due to the band gap of the silicon material used in the solar cells. Analyses were carried out using values of the atmospheric optical

absorption coefficients in the $450 - 1100\ nm$ wavelength range that were reported by Moon [4]. The coefficients ranged between 0.05 and 0.96 per air mass. The spectral response of the solar cells peaked at about $850\ nm$ where the atmospheric optical absorption was about 0.1 per air mass. The geometrical air masses used by Zoutendyk must be multiplied by 0.7 to correct for the 7.4 kft altitude [5]. For $\alpha = 0.1$ per air mass and $m = 0.7$, the exponential term in Equation 8, has a value of about 0.93. At the largest and smallest values of the optical absorption coefficient, 0.96 and 0.05 per air mass, the values of the exponential term will be 0.51 and 0.96, respectively. Clearly the exponential term varies with wavelength when Moon's atmospheric optical absorption coefficients are used in Equation 8. However, as shown in Equation 7, the exponential term is convoluted with the cell spectral response. The spectral response is always less than one; it decreases from a maximum value at $850\ nm$ to approximately zero at the cut off wavelengths. The effect of convolution of the spectral response with the exponential term in Equation 7 is to decrease the weighting of the exponential term in the integral. A non-constant exponential term in Equation 7 will produce a concave up feature in Langley plots [4]. There is no evidence of a concave up feature in the Langley plots in Zoutendyk's work. This suggests variations in the atmospheric optical absorption coefficients were small enough so as to not invalidate the use of Langley plots to determine solar cell AM0 short-circuit currents.

It is surprising the extrapolated AM0 short-circuit currents agree with the space measurements to within 2 %. It may be the case that the optical absorption coefficients used by Zoutendyk are not appropriate for the conditions under which the mountaintop measurements were carried out. There are three reasons for this conjecture.

1. The ratios of Zoutendyk's measured and calculated short-circuit currents as a function of air mass differ considerably. He used Equation 7 to calculate short-circuit currents along with a standard AM0 spectral irradiance [5], the spectral response of the cells and atmospheric optical absorption coefficients [6]. In every case, the calculated short-circuit currents are smaller than the ones measured, suggesting the atmospheric optical absorption coefficients used are larger than the effective optical absorption coefficients at 7,400 ft.

2. The irradiances measured as a function of air mass are also considerably larger than the irradiances calculated using Equation 5. Zoutendyk plotted measured irradiance as a function of air mass on semi-log plots. The curves are clearly concave up providing convincing evidence of the effect of non-constant atmospheric optical absorption coefficients. In the case of the irradiance curves, Equation 5 shows the integral extends over a larger wavelength range and is not convoluted with the cell spectral response. The larger wavelength range and absence of the convolution both lead to the full effect of the atmospheric optical absorption coefficients on the transmitted sunlight and a concave up feature in irradiance plots.

3. An analysis of Zoutendyk's data in six Langley plots yields atmospheric optical absorption coefficients ranging between 0.079 and 0.101 per unit air mass; the average is 0.087 per unit air mass. The average value of Moon's optical absorption coefficients is about 0.15 per unit air mass in the 700 to $900\ nm$ range where the solar cell spectral response is the largest. The fact that the average slope is about 60 % of Moon's optical absorption coefficients suggests either Moon's coefficients are too large to be used in predicting AM0 short- circuit currents or the atmospheric conditions that prevailed during Zoutendyk's measurements are different than the conditions under which Moon's coefficients were determined. Additionally, the variation in the slopes of the Langley plots measured from day-to-day suggests changing atmospheric conditions may have played a role in the mountaintop measurements.

Ritchie recognized the problems associated with using Moon's atmospheric optical absorption coefficients to correct solar cell short-circuit currents. He employed measurements on a mountaintop to produce secondary standards [7] that did not employ Langley plots. The secondary standards were based on the use of primary standards calibrated with the balloon method and the following equation:

$$I^{s}_{sco} = \frac{I^{p}_{sco}}{I^{p}_{scm}} \times I^{s}_{scm} \tag{10}$$

where I^{s}_{sco} and I^{p}_{sco} are the calculated secondary and measured primary standard AM0 short-circuit currents, respectively; I^{s}_{scm} and I^{p}_{scm} are the secondary and primary standard short-circuit currents, respectively, measured at the same time on a mountaintop. The balloon method was used to measure I^{p}_{sco}. Following the mountaintop measurements, the secondary standards were flown on a balloon flight and the AM0 short-circuit currents measured; the currents agreed to within 0.5% with the currents predicted using the mountaintop measurements based on Equation 10. It is important to note that the spectral responses of the primary and secondary standards must be the same when using a primary balloon standard, Equation 10 and mountaintop measurements to produce secondary standards.

Aircraft method

The use of an aircraft to carry out high-altitude solar cell measurements at altitudes between 47 kft and 6 kft and air masses in the 0.180 – 0.862 range was first reported by Brandhorst [8]. It was suggested that the aircraft method is attractive when compared to the mountaintop method for three reasons. First, measurements are made at lower values of air mass than the mountaintop method resulting in shorter extrapolations of the short-circuit current on Langley plots. It is expected that the more accurate values of the AM0 short-circuit currents will be obtained if the extrapolation is over a smaller range of air masses. Second, the atmosphere should be less prone to compositional changes during the relatively short time of the aircraft measurements as compared to diurnal mountaintop measurements, i.e., minutes versus hours. Third, the measurements are made at altitudes that are above ground haze and low-altitude atmospheric disturbances.

The aircraft method employed a 4.5” diameter windowless collimator with a collimation ratio of 4:1 that was mounted inside the aircraft and extended through a hole in the side of the tail section [9]. The collimator was designed to over-fill the cell holder so that the cells were uniformly illuminated even when the orientation of the aircraft resulted in a $\pm$2-degree error in the pointing of the collimator. The collimator angle was set before each flight to the zenith angle of the sun during the measurements. The tail section was not pressurized and the cells were exposed to the low pressure and temperature environment that is characteristic of the altitudes at which the measurements were carried out. Single-junction silicon solar cells were mounted on a heated stage and the cell temperature maintained between 15 and 30 ^{o}C with a variation of less than 4 ^{o}C. The cell short-circuit current was taken as the current through a 1.000 Ω precision resistor that was placed in series with the cell, as was done by Zoutendyk. The aircraft altimeter was used to measure pressure to an accuracy of 75 ft. The pilot used a sight tube mounted next to the controls in the cockpit to orient the aircraft and control the pitch, roll and yaw so as to point the collimator at the sun with a pointing accuracy of better than $\pm$ 2 degrees. Altitude, cell short-circuit current and cell holder temperature were measured at altitude intervals of 5 kft during descent from 47 to 6 kft.

A standard atmospheric model was used to convert the altitude measurements to pressure [5]. The air mass was calculated using:

$$m = \left(P / P_o\right)\sec\theta \tag{11}$$

where P is the pressure at which the cell short-circuit current was measured and P_o is the sea-level pressure. Langley plots were produced and extrapolations carried out to determine the AM0 short-circuit current of the single-junction silicon solar cells. The AM0 short-circuit currents were corrected for cell temperature, precision resistor temperature, ozone absorption and the earth-sun distance. The extrapolated AM0 short-circuit current was corrected for ozone absorption using the cell spectral response; ozone absorption coefficients in the $400 - 700\ nm$ wavelength range [10]; ozone altitude profile [11]; and the percent of the total column ozone above the aircraft during measurements. The effect of ozone absorption on the short-circuit current of single-junction Si and GaAr solar cells was estimated to be 1.04 and 1.23 %, respectively. Brandhorst reported that

all the Langley plots were straight lines [8,9]. However, there were differences in the slopes of the Langley plots from flight-to-flight suggesting atmospheric conditions, while perhaps constant during a flight, changed from flight-to-flight. The atmospheric optical absorption coefficients, as determined from the slopes of the Langley plots in the publications, ranged between 0.09 and 0.30 per air mass. The change in the slopes suggests there were variations in the concentration of optically absorbing atomic and molecular species in the atmosphere from flight-to-flight. The agreement in the AM0 short-circuit currents, measured by the aircraft method and the mountaintop method that used Equation 10, was $\pm$ 0.9 %. The AM0 short-circuit currents measured during three separate flights were reproducible within $\pm$ 1 % even though the slopes of the Langley plots, and therefore the atmospheric conditions, were different.

Hadley analyzed data from three single-junction silicon cells. Two were balloon calibrated primary standards and one was a secondary standard calibrated using mountaintop measurements with Equation 10. All three of the cells were characterized with the aircraft method. He found that the cell AM0 short-circuit currents measured by the aircraft method were consistently about 1.6 % lower [12]. Hadley pointed out that the Langley plots for different days had different slopes and some of the plots appeared to be concave up . While there was a need to make spectral corrections because the spectral responses of the cells were slightly different, it was not possible since the different slopes for different days “indicate that there cannot be a unique value of the spectral correction factor.” The effect of Hadley’s work was to suggest that while it was agreed that the use of the Langley plots in the mountaintop method was faulted, there was evidence that there were also problems in using Langley plots to analyze data from the aircraft method.

Subsequently, the aircraft method was used to measure silicon single-junction solar cell short-circuit currents versus altitude. The measurements resulted in Langley plots that exhibited an anomalous behavior. [13]. The plots had a curve with two linear regions, each of which had a different slope. There was a “break” in the curve where the linear segments met. It was determined that the “break” occurred at an air mass that corresponded to the altitude of the tropopause. The short-circuit currents measured at altitudes above the tropopause produced a linear plot with a larger slope than the slope of the currents measured at altitudes below the tropopause. Extrapolation of each of the linear segments produced different AM0 short-circuit currents. The Langley plots for data collected at altitudes above the tropopause extrapolated to larger AM0 short-circuit currents than the plots for data collected at altitudes below the tropopause. The slopes of the Langley plots for data collected above the tropopause were the same on a month-to-month basis while the slopes for data collected below the tropopause were different on a month-to-month basis. The observation that the slope above the tropopause was constant on a month-to-month basis suggests the concentrations of the optically absorbing atomic and molecular species are the same on month-to-month basis for species that absorb in the region of the solar spectrum that contributes to cell current [13]. The atmospheric optical absorption coefficient determined from one of the Langley plots for the data collected above the tropopause was about 0.20 per air mass. On the other hand, the fact that the slopes below the tropopause changed on a month-to-month basis suggests concentrations of the absorbing atomic and molecular species are different below the tropopause on a month-to-month basis. The atmospheric optical absorption coefficient determined from one of the Langley plots for the data collected below the tropopause was about 0.09 per air mass.

A comparison was made of AM0 short-circuit currents of five silicon single-junction solar cells measured with the balloon and aircraft methods [13]. The accuracy of the balloon measurements was estimated at $\pm$ 0.9 %. Only aircraft data collected above the tropopause were used. Differences in the AM0 short-circuit currents measured by the two methods ranged from 0.3 to 1.2 % with an average of 0.7 %. The AM0 short-circuit currents measured with the aircraft method were always larger than those measured with the balloon method. It was concluded that the measurements “show excellent agreement”, and the aircraft method must be used above the tropopause in order to produce good results.

Brandhorst carried out a series of experiments with the aircraft method to determine the wavelength region of the anomalous effect [14]. Optical filters were placed over solar cells and data collected both above and below the tropopause. The Langley plots had straight lines for data collected with filters that transmitted red and green light; an anomalous plot with a “break” was produced with data collected with a filter that transmitted blue light. The measurements suggested the anomalous effect was due to an atomic or molecular species that absorbed in the blue wavelength region of the solar spectrum, and that the species existed primarily above the tropopause.

The anomalous Langley plot can be understood by modifying Equations 7, 8 and 9 to include the effect of two atmospheric optical absorption coefficients. The atmospheric optical absorption coefficient for an optically absorbing species that exists primarily above the tropopause is taken as $\alpha 1$ for a range of wavelengths from $\lambda 1$ to $\lambda 2$, the wavelength range where the spectral response contributes to the cell current. The optical absorption coefficient in the same wavelength range is $\alpha 2$ for a different species that exists primarily below the tropopause in the same range of wavelengths. Equations 7, 8 and 9 above the tropopause become:

$$I_{scm} = e^{-\alpha 1 m} \int_{\lambda 1}^{\lambda 2} R(\lambda) S_o(\lambda) d\lambda = e^{-\alpha 1 m} I_{sco} \quad \text{and}$$

$$Log_{10} I_{scm} = -0.4343 \alpha 1 m + Log_{10} I_{sco} . \tag{12}$$

The slope of the Langley plot above the tropopause is $-0.4343\alpha 1m$ and the extrapolated AM0 short-circuit current is I_{sco}. Below the tropopause:

$$I_{scm} = e^{-\alpha 2 m} \int_{\lambda 1}^{\lambda 2} R(\lambda) S_{ot}(\lambda) d\lambda = e^{-\alpha 2 m} I_{s\cot} \quad \text{and}$$

$$Log_{10} I_{scm} = -0.4343 \alpha 2 m + Log_{10} I_{s\cot} \tag{13}$$

where $S_{ot}(\lambda)$ is the solar spectral irradiance just below the tropopause; it is corrected for absorption due to the optically absorbing species above the tropopause. $I_{s\cot}$ is the short-circuit current due to the convolution of $S_{ot}(\lambda)$ with $R(\lambda)$. The slope of the Langley plot below the tropopause is $-0.4343\alpha 2m$ and the extrapolated AM0 short-circuit current is $I_{s\cot}$. The "break" in the straight line segments on the Langley plot defines two regions of air mass where the data have linear characteristics, namely, a straight line segment with a larger slope at lower air masses and a straight line segment with a smaller slope at larger air masses. It follows that $\alpha 1$ in the region of lower air is greater than $\alpha 2$ in the region of larger air masses. Hence, the anomalous plots may be explained by assuming the atmospheric optical absorption coefficients are different above and below the tropopause.

The aircraft method has been developed over the years by investigators at NASA Glenn Research Center [15,16]. A large body of calibration data has been collected and AM0 standards provided to the PV community. The aircraft has been replaced twice and the method improved. The current aircraft is a Lear 25 that houses the instrumentation and collimator in a pressurized and temperature controlled compartment. Photographs of the Lear 25 aircraft, collimation tube and test cell may be viewed on the NASA Glenn Research Center Web site [17]. The ratio of the collimation has been increased to 1:4.5. The method was upgraded to carry out measurements every nine seconds during a 6E-4 air mass per second rate of descent from 50 kft down to the tropopause. Sources of random error were estimated to be about 0.04 % and agrees with measurements. The difference in the average of measurements on a single-junction cell carried out over a twenty-year period and a recent measurement was at the 0.05 % level. Systematic errors were estimated to be at the one percent level. Space shuttle AM0 short-circuit current measurements on two cells were compared with the aircraft method. The aircraft measurements were less than the shuttle measurements by 1.0 and 0.8 % for the two cells; the errors were consistent with the estimated systematic errors.

The role of ozone on the solar cell AM0 short-circuit current measured with the aircraft method has been investigated by Snyder and collaborators [18]. The extrapolated AM0 short-circuit current was corrected using an ozone correction factor. The correction factor was determined using a calculated AM0 short-circuit current

and a calculated short-circuit current that included the effects of ozone absorption. The WMO solar spectral irradiance [19] and solar cell spectral response were convoluted using Equation 1 to calculate the AMO short-circuit current I^x_{scoc} where x corresponds to Si, GaAs and InGaP single-junction solar cells. The short-circuit current I^x_{scdu} was calculated using Equation 7 and the WMO solar spectral irradiance, solar cell spectral response, ozone absorption coefficients [20] and total column ozone value T_{co}. The ozone correction factor F^x_o for each of the types of solar cells was found using:

$$F^x_o = \left(\frac{I^x_{scoc} - I^x_{scdu}}{I^x_{scdu} T_{oc}} \right) \tag{14}$$

where the units of T_{co} are Dobson units, d.u. The correction factors were found to be insensitive, at the 5 % level, to the value of the total column ozone, different sets of spectral response data, and the resolution of the spectral response data used in the calculations. The ozone correction factor was reported to increase with an increase in the optical band gap of the materials used in the solar cells.

The ozone correction method consisted of employing a Langley plot to first determine the extrapolated AM0 short-circuit current I^x_{scol}. Then the current was corrected for optical absorption in the ozone column on the day of the flight. The sun zenith angle, total column ozone on the day of the flight and the ozone correction factor were used in the following equation to determine the AM0 short-circuit current for the various types of cells:

$$I^x_{sco} = I^x_{scol} + 0.83 F^x_o T_{oc} \sec\theta \,. \tag{15}$$

The 0.83 factor results from assuming that 83 % of the total column ozone was above the aircraft during the measurements. The correction method was used to analyze Si solar cell data collected during 20 flights. The correction resulted in an increase of 0.52 % in the Si AM0 short-circuit current as compared to the earlier one percent correction method introduced by Brandhorst [9]. Applying Equation 15 to the earlier aircraft measurements also reduced the differences noted by Hadley in currents determined with the aircraft and balloon methods [12]. The percentage standard deviation of the ozone corrected currents decreased from 0.49 % with the earlier correction method to 0.28 %, thereby suggesting the importance of using Equation 15 to correct for the effect of ozone.

Applying the correction method to a GaAs solar cell, which has a larger band gap than Si, resulted in AM0 short-circuits that were different from flight-to-flight. The corrected currents increased with increases in total column ozone suggesting that the method was sensitive to the band gap of the cell. The correction method was revised in an effort to eliminate the dependence of currents on total column ozone [21]. The revised method called for first correcting the short-circuit current measured at each altitude for ozone absorption, then plotting the data and extrapolating to air mass zero. The approach requires the column ozone at each of the altitudes at which the cell current is measured. The TOMS standard ozone profiles were used to calculate column ozone as function of altitude [22]. Figure 2 shows the TOM ozone profiles used in calculating the column ozone. The average ozone density in the figure is plotted at the midpoint of each Umkehr layer [23], starting at layer zero corresponding to an altitude of 9 kft, through layer 9 at 143 kft. The density shown in

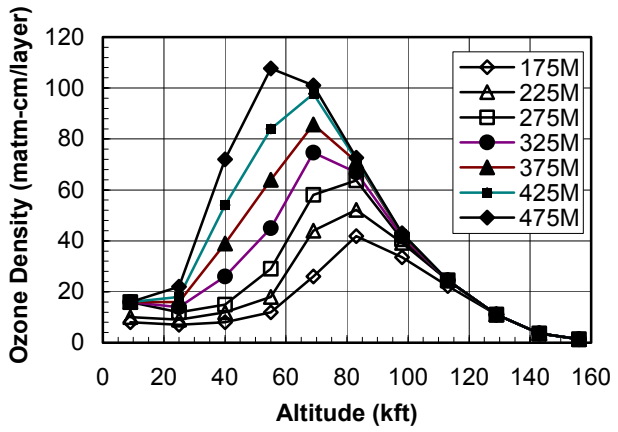

Figure 2. TOMS ozone profiles as function of altitude and total column ozone at mid latitudes [22] .

the figure at 156 kft includes the ozone above 156 kft. The profiles in the figure are for mid latitudes and total column ozone values ranging from 175 to 475 d.u. Mid latitudes are around 45 degrees north, the latitude of the NASA Glenn Research Center flights. The maximum altitude for the flights is about 50 kft. Figure 2 shows the fraction of the total column ozone above 55 kft decreases with increasing total column ozone. The fraction at 55 kft is about 0.87 of the total column ozone when the total column ozone is 175 d.u.; the fraction decreases to about 0.77 at 475 d.u. The fraction is about 0.92 and fairly independent of total column ozone at 40 kft.

The revised AM0 short-circuit current correction method included converting the aircraft altitudes to atmospheric pressure, p . The total column ozone on the day of the flight was obtained and used to select the appropriate TOMS ozone profile in Figure 2. The fraction of the total ozone column $f(p)$ above the aircraft during each of the measurements was calculated. The ozone corrected short-circuit current $I_{scm}(p)$ was calculated for each measurement $I_{sc}(p)$ using:

$$I_{scm}(p) = I_{sc}(p) + f(p)F_o^x T_{oc} \sec\theta \tag{16}$$

The ozone corrected short-circuit currents were plotted as a function of pressure on a Langley plot, instead of a function of air mass. The linear plot was extrapolated to zero pressure to determine the AM0 short-circuit current. Results with the revised method were compared to the one percent method using data for a Si single-junction solar cell. Data collected over two time intervals, namely a short term and long term, were compared. The short-term data were collected on one cell during twenty flights in one year. The long-term data were collected on the same cell during thirteen flights over a period of eight years. Table 1 shows differences in the average AM0 short-circuit currents using the one percent, Av. Isco 1%, and revised ozone correction methods, Av. Isco Revised. The percentage difference in the averages of the currents are 0.52 and 0.54 % for the short and long terms, respectively, showing the percentage differences are essentially the same for the two periods. The percent standard deviation decreases from 0.49 to 0.26 % and 0.72 and 0.48 % for the short and long terms, respectively, showing the importance of the revised ozone correction method in reducing the systematic error in the aircraft method. The percentage differences between the highest and lowest AM0 short-circuit currents decreases from 3.2 to 1.2 % and 2.5 to 1.0 % for the short and long terms, respectively, again showing the improvement of the results with the revised ozone correction method. The relatively larger percentage differences in the highest and lowest AM0 short-circuit currents is due to the fact that the zenith angle ranged between about 48 and 68 degrees during the various flights. Both methods show a decrease in the ozone corrected AM0 short-circuit currents as the zenith angle increases. However, the revised ozone correction method is considerably more effective in correcting for the effect of the zenith angle. Not shown in Table 1 is the percentage difference in the average AM0 short-circuit currents using the revised method for the short and long terms; the difference is 0.26 % which is within the standard deviation for the measurements.

Table 1. Comparison of ozone correction methods for Si, GaAs and InGaP single-junction solar cells [21].

Si Short Term		
Av. Isco Revised - Av. Isco 1%=0.52%		
	1%	Revised
	(%)	(%)
Std. Dev.	0.49	0.26
High-Low	3.2	1.2
Si Long Term		
Av. Isco Revised - Av. Isco 1%=0.54%		
	1%	Revised
	(%)	(%)
Std. Dev.	0.72	0.48
High-Low	2.5	1.0
GaAs Long Term		
Av. Isco Revised - Av. Isco 1%=1.0%		
	1%	Revised
	(%)	(%)
Std. Dev.	0.75	0.47
High-Low	2.6	2
InGaP		
Av. Isco Revised - Av. Isco 1%=2.3%		
	1%	Revised
	(%)	(%)
Std. Dev.	0.45	0.14

Table 1 also shows the differences in the average AM0 short-circuit currents for GaAs and InGaP single-junction solar cells using the 1%, and revised ozone correction methods. The GaAs data were measured in 31 flights over a nine-year period. The InGaP data were collected during seven flights over a few years. The band gap of GaAs is 1.43 eV. The band gap of the InGaP cell is not known because the alloy concentrations were not reported for this particular cell; however, it is expected that it is greater than the band gap of GaAs. The percentage difference in the averages of the currents corrected by the 1% and revised methods are 1.0 and 2.3 % for the GaAs and InGaP

cells, respectively, showing the revised method gives larger currents as the band gap increases. The percent standard deviations are reduced for both the cells as was observed for the Si cell, again confirming the importance of the ozone correction. The differences in the high and low current values are reduced for both cells when the revised method is used. A larger zenith angle results in a larger correction in the AM0 short-circuit currents for both cells. The revised method is more effective in correcting for larger zenith angles as is illustrated by the smaller high-low percentage differences in the AM0 short-circuit currents. However, there is a trend for corrected currents to exhibit a decreasing trend with increasing zenith angle.

Balloon Method

The first balloon method measurements to determine the AM0 short-circuit current of single-junction silicon solar cells was reported by Zoutendyk [24]. A sun tracker weighing about 70 lbs was flown mounted on the top of a balloon, as opposed to in a gondola suspended below the balloon. Mounting the sun tracker on top of the balloon also reduced the effect of sunlight reflections from the balloon on the cell measurement. The top mounting also eliminated anticipated complicating effects of pendulum and torsional motion of the gondola on tracking of the sun. The downlinked data included three solar cell temperatures, fourteen cell short-circuit currents and seven precision standard voltages. The cell short-circuit current was defined at the current through a 1.000 Ω precision resistor that was placed in series with the cell. The weight of the balloon, parachute, sun tracker, batteries, transmitter, data acquisition system and other incidental items was 425 lb; the batteries and transmitter were mounted in a gondola attached to the parachute which is turned was attached to the bottom of the balloon. The maximum volume of the balloon was 175,000 cubic feet and required 7,150 cubic feet of helium to provide an ascent rate of about 1000 feet per minute. It took about two hours for the balloon to reach the 80,000 ft float altitude. The float time for flights was about four hours with two hours of floating time before solar noon and two hours after solar noon. Two vehicles were used in support of flights. One was a bus with communications equipment that maintained a distance of less than 200 miles from the balloon and received the downlinked data. The other vehicle was a chase truck that retrieved the equipment and solar cells. An aircraft was also available to assist if necessary with tracking the balloon.

The solar irradiance at a zero zenith angle and the 80 kft float altitude was estimated to be 95 % of AM0, corresponding to an air mass of 0.05. A reduction of 0.3 % was estimated in the air mass 0.05 cell short-circuit current, as compared to AM0, considering the spectral response of the solar cells. The sun tracker was able to track the sun to within $\pm$ 4 degrees. An error analysis of the measurement system showed a maximum error of about $\pm$ 0.6 %. Three flights were carried out over a period of three months and the results of the calibration of two silicon solar cells were reported. The cell temperatures were 19 $\pm$ 1 ^{o}C during the first flight and 32 $\pm$ 1 ^{o}C during the last two flights. The data were corrected for temperature. AM0 short-circuit currents were reported for the mean earth-sun distance and 28 ^{o}C cell temperature. No corrections were made for ozone absorption. The repeatability in AM0 short-circuit currents for three flights was better than $\pm$ 0.5 % and the accuracy estimated at $\pm$ 0.6 %.

The balloon method has been further developed over the years by Anspaugh and collaborators [25]. It has been used by the NASA Jet Propulsion Laboratory to provide primary standards to the space photovoltaic community. The standards are calibrated at about 120,000 ft, the float altitude of the balloon. Balloon flights are carried out at least once a year during the summer months. The combined weight of the balloon and top and bottom payloads is about 1,400 lb. The main balloon has a volume of about 3.6 E6 cubic feet and requires about 24,000 cubic feet of helium. Launching requires the use of a tow balloon, spool vehicle, launch vehicle and helium tanker. The top payload weighs about 140 lb and consists of the sun tracker, solar panel, transmitters, command receivers, data acquisition electronics, video camera, batteries and miscellaneous items. The bottom payload is tethered in a gondola and includes of batteries, ballast module, flight terminate equipment, pressure transducer, transmitters, GPS receivers, and a variety of supporting electronic systems. The top and bottom payloads have separate parachute and release mechanisms. In excess of 75 cells and modules can be calibrated during a flight. An on-board microprocessor-based system is used for data acquisition and storage during flights. Current-voltage measurements are made over a voltage range from about 100 mV to the cell open-circuit voltage. Cell temperatures are measured both during ascent and at float altitude. Cell temperatures are between 30 and 40 ^{o}C during ascent and about 75 ^{o}C at float altitude. The balloon ascent rate was about 900 ft/min and the time from launch to a 120 kft float altitude was about two

hours; float times ranged between 1.5 to 3.0 hours. Data are downlinked to a base station at the launch site. An aircraft with a two-person crew direct both the termination of the flight and recovery activities. The aircraft crew in retrieving the two payloads directs a chase truck equipped with communications equipment.

Laboratory characterization of solar cells and modules is carried out both before and after balloon flights to insure the cells are not damaged. Cells with a variety of structures have been flown including single and multi-junction cells fabricated from crystalline and amorphous materials. Both thick crystalline and thin-film cells have been calibrated. Only data collected with the tracker pointed to within ± 2 % of the sun are used in characterizing cells. "Wild" data points have been observed in recent years with modifications in the equipment, e.g., adding a video camera and placing some of the transmitters in the top package [26]. The data acquisition system has been programmed to exclude "wild" data points from the data files that were used in determining the cell AM0 characteristics. The cause of the "wild" points was not know but it was suggested that they may be due to water condensation or radio interference.

A module was flown for 41 flights to evaluate both measurement repeatability and the role of position on the solar panel. It was felt that changing the position of the module on solar panel could be used to evaluate the geometric quality of the solar irradiance "with regard to uniformity, shadowing, or reflections" [27]. The standard deviation for 41 flights was 0.46 % and it was concluded that there are no geometric problems. The cell used in the 41 flights was damaged and replaced. It was replaced with a set of nine standard cells and modules to continue checking the repeatability of the balloon method. The nine standard cells and modules were not flown on every flight. Cells and modules were flown between 6 and 26 times. The standard deviations of the AM0 short-circuit currents for the flights range between 0.23 and 1.0 %. The percent differences between the maximum and minimum AM0 short-circuit currents range between 1.3 and 4.4 % for all the standard cells [28]. Two of the silicon single-junction standard cells were flown on the Discovery Shuttle and the AM0 short-circuit current measured in a manner similar to the balloon method. The differences between one measurement on the shuttle flight for each of the two cells, and the average of the AM0 short-circuit currents measured on multiple balloon flights, were 0.21 and 0.11 %, respectively. The agreement is seen as "verifying the accuracy of the calibration procedures used on the balloon flights" [29].

The agreement between shuttle and balloon calibrations for two Si solar cells was 0.21 and 0.11 %, yet the set of standard cells have standard deviations for multiple balloon flights that range between 0.23 and 1.0 %. Moreover, the percentage differences between the maximum and minimum AM0 short-circuit currents range between 1.3 and 4.4 % for the set of nine standard cells [28]. If the agreement between the shuttle and balloon methods is taken as representative of the accuracy of the balloon method for silicon single-junction cells, then the differences in the balloon measurements may be due to either the spectral responses or instabilities in the standard cells. The cell structure and materials are not given for the nine standard cells [28], and for this reason, it is not possible to correlate the differences with cell spectral response. The standard cell with a 1.0 % standard deviation and a 4.4 % difference between the maximum and minimum AM0 short-circuit current was flown on 13 balloon flights. The data may be used to evaluate the role of cell instability on measurements. The first current measurement was 166.83 mA; the current measured on the thirteenth flight was 611.11 mA. Inspection of the measurements for the 13 balloon flights shows the trend is for the cell current to decrease with each successive flight. The data show that the reason for the relatively large cell statistics is a gradual decrease in the cell's current. The behavior suggests the existence of a cell degradation mechanism. It in noteworthy that the cell operates at 75 ^{o}C at the float altitude. The cell will operated at 75 ^{o}C in excess of twenty hours during the 13 flights. It is probable that thermal degradation resulted in the relatively large change in cell current. However, opto-electronic degradation and other sources of instability should also be considered.

SUNTRACKER PROJECT

A joint NASA Glenn Research Center/Wayne State University program called Suntracker is underway to explore the use of weather-balloon and communication technologies to characterize solar cells at elevations up to 120,000 feet [30-32]. The balloon flights are low-cost and can be carried out any time of the year.

The Suntracker scientific package includes a collimator with a cell to be calibrated, two GPS receivers, two transmitters, two separate battery packs, control electronics and a video camera. Figure 3 shows the scientific package. The main body of the package is cylindrical and fabricated from urethane foam; it measures 11" in

Figure 3. Suntracker scientific package developed for characterizing multi-junction solar cells in the stratosphere.

Table 2. Summary of Suntracker Flights

ST	Date	Launch Site	Landing Site	Alt. (ft)	Range (mi)
I	8/29/99	Findlay, OH	Marion, OH	87,000	40
II	9/9/00	Findlay, OH	Aborted due to hardware problems		
III	9/14/02	Findlay, OH	Greenwich, OH	94,256	55
IV	10/12/02	Findlay, OH	Brunswick, OH	87,127	94
V	11/9/02	Portland, IN	Aborted due to surface winds		
VI	12/7/02	Portland, IN	Canton, OH	95,956	186
VII	8/16/03	Findlay, OH	Amlin, OH	99,500	68

diameter and 11” high. The package is about one inch thick and provides thermal insulation for the electronics. Two battery packs are supported 22” from the main body by light carbon composite tubes that are arranged in a “z” configuration. The battery packs are mounted in this fashion to increase the rotational inertia of the package; the 22” length is limited by the interior width of the mobile unit. The two battery packs are enclosed in separate carbon tubes and wrapped in foam insulation to provide thermal insulation. The dimensions of the collimator are 1.25"x1.25"x4.00"; the front aperture is 1.00"X1.00" and the cell area 0.79"x0.79" [x]. The dimensions of the collimator were selected to provide a 1:4 collimation ratio and a one degree pointing accuracy. The collimator prevents light scattered from the balloon, earth, moon or clouds from contributing to solar cell current . Two motors and supporting electronics control the altitude and bearing angles of the collimator during a flight. A video camera is mounted on top of the package and used to observe the operation of the Suntracker as it ascends though low temperatures to the stratosphere. The weight of the payload is about six pounds. Photographs showing the system components inside the scientific package may be viewed on the Suntracker Web site [33].

The scientific package is attached to a parachute that is affixed to a latex balloon. The balloon weighs about three pounds and is inflated with about 250 cubic feet of helium and launched by a three-person team. The Suntracker scientific package is tethered below the balloon and the electronics is programmed to point the collimator at the sun during ascent. The balloon ascends at a rate of about 800 ft/min to a burst altitude ranging between about 87 and 100 kft in about two hours and then parachutes to a landing site. Data are downlinked continuously during the flight on 2 m and 70 cm bands to a mobile unit that is equipped with receivers, computers and tracking software. The three-person team in the mobile unit chases the balloon, records the data and retrieves the scientific package. The data includes cell voltage, cell temperature, electronics module temperature, video, reference voltage, and atmospheric pressure. The short-circuit current is determined from the cell voltage across a 1.000 Ω precision resistor that is in series with the cell.

RESULTS

Seven flights have been attempted with five successful launches. Table 2 shows the launch dates and locations, burst altitudes, landing sites and balloon trajectory ranges. The scientific package was retrieved on the same day for the Suntracker I, III and IV flights. Hardware problems developed during the Suntracker VI and VII flights that resulted in the loss of GPS signals; the package was found within a few days of the launch by individuals and subsequently retrieved. A single-junction silicon solar cell was mounted in the collimator during

the flights. The cell voltage data downlinked during the Suntracker IV and VI flights have been analyzed using Langley plots to determine the AM0 short-circuit current. The Suntracker IV uncorrected short-circuit current versus altitude is shown in Figure 4. Only the maximum currents were selected for use in the Langley plot. The cell current data illustrate the tracking characteristics during the ascent. For the most part the Suntracker was not locked on the sun during the flight. The video data showed the motors slowed down during the ascent as a result of the low atmospheric temperatures. Motor assemblies using lubricant with lower temperature specifications will be evaluated in future flights. Additionally, the stability of the scientific package and the collimator control algorithm will be investigated in order to improve the performance of the Suntracker system.

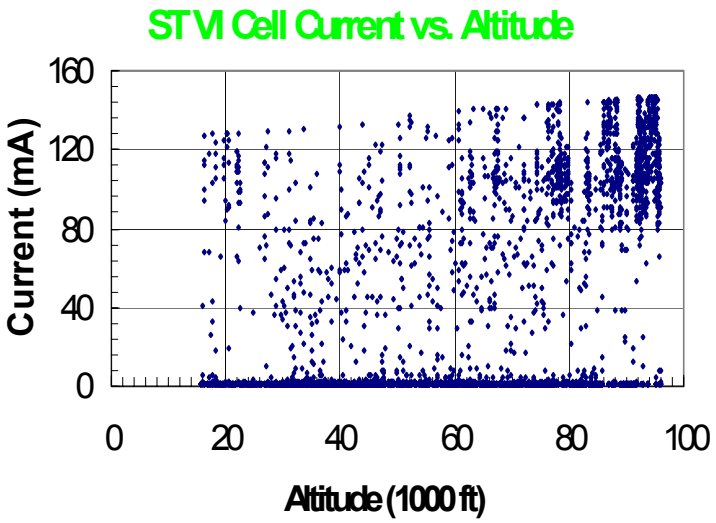

Figure 4. Suntracker VI short-circuit current versus altitude for a single-junction silicon solar cell.

The cell temperature versus altitude during the Suntracker VI flight is shown in Figure 5. Also shown are the radiosonde data reported by the National Weather Service (NWS) on the day of the flight. The effect of solar heating on the cell current is apparent . While the solar cell temperature increased from –10 to about 0 °C as the balloon ascended from 80 to 96 kft, the atmospheric temperature remained at about –45 °C. The dependence of the cell and NWS temperatures in this altitude range suggests that the cell temperature may be higher at higher altitudes. If this is the case, it will be possible to operate cells closer to 25 °C at higher altitudes, and to determine the temperature coefficient of the short-circuit current as the package ascends.

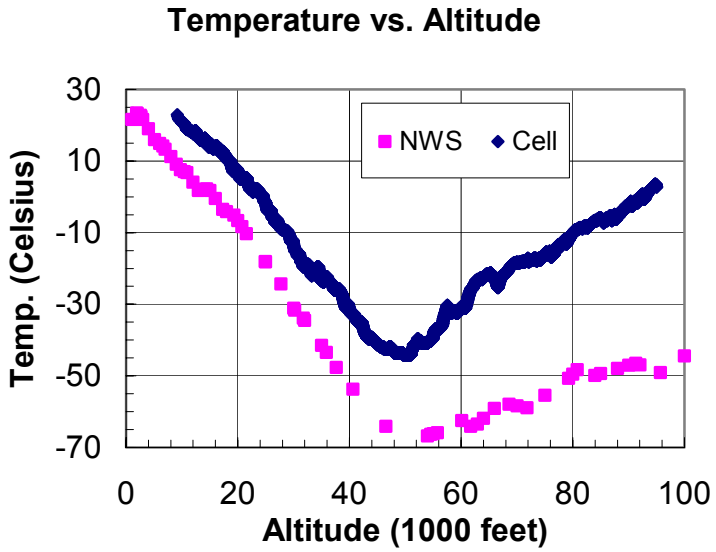

Figure 5. Suntracker VI downlinked solar cell and atmospheric NWS temperatures versus altitude.

Figure 6 is a Langley plot of the data for a single-junction silicon solar cell from the Suntracker IV and VI flights. The optical air masses were calculated using Equation 11. The data have been corrected for the earth-sun distance and cell temperature, and fit with straight lines. The extrapolated AM0 short-circuit currents are 144.32 and 144.38 mA for the Suntracker IV and VI measurements, respectively. The average AM0 short-circuit current is 144.35 mA ± 0.02 %. The resolution of the eight-bit ADC in the Suntracker data acquisition system is ± 0.2 %, showing that the agreement between the two flights is better than the uncertainty in the measurements and probably reflects the statistics of the curve fitting etc. The AM0 short-circuit current of the single-junction silicon solar cell flown on the Suntracker flights was determined using the aircraft method at NASA Glenn Research Center [21]. The AM0 short-circuit current was 144.88 mA and within ± 0.36 % of the Suntracker average value. The results agree to within the statistics

of the two methods, namely about ± 0.2 % for the Suntracker measurements and ± 0.6 % for the aircraft method.

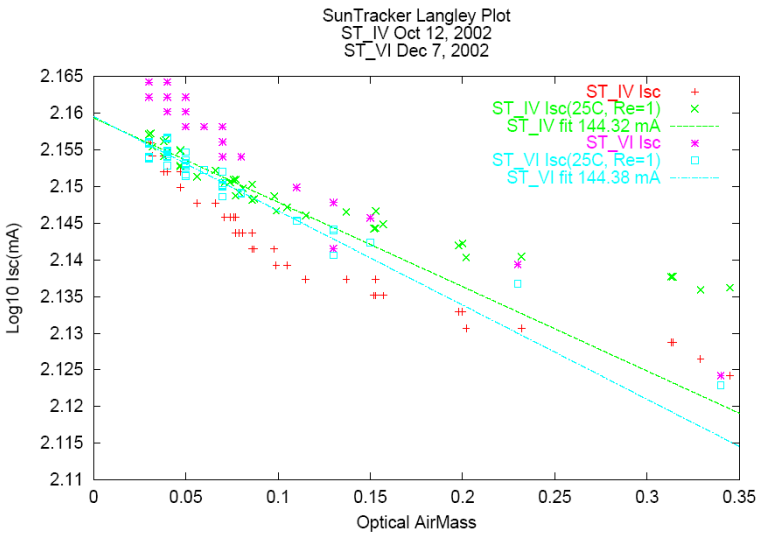

Figure 6. Langley plot of corrected Suntracker IV and VI data for a single-junction silicon solar cell.

It is instructive to determine the atmospheric optical absorption coefficients for the two methods using Equation 9. The slopes of the two straight lines in Figure 6 were analyzed to determine the absorption coefficients; the coefficients are 0.265 and 0.293 per air mass for the Suntracker IV and VI data, respectively. The average value of the atmospheric optical absorption coefficient is 0.280 per air mass ± 5 %. An analysis of the Langley plot produced with aircraft data gives absorption coefficients of 0.125 per air mass. The Suntracker value is somewhat larger than the 0.20 per air mass determined from the earlier aircraft measurements [13] while the absorption coefficients determined with the current aircraft data is considerably less. The reasons for these differences are not understood and will be the subject of future investigations.

CONCLUSIONS

The voltage dependence of the spectral responses of multi-junction solar cells complicates optimization of cell design. The series nature of multi-junction solar cells places more demands on the need for standard cells characterized under AM0 conditions. Cells selected for use as standards should have a history of thermal cycling and light soaking that provides evidence of the level of cell stability. The AM0 short-circuit current of a single-junction silicon solar cell was determined using data collected during two Suntracker flights. The agreement in the two measurements was ± 0.02 %. The agreement in the AM0 short-circuit current of the cell measured with the Suntracker balloon method and NASA Glenn Research Center aircraft method was ± 0.36 %, which is within the uncertainty of the two methods. There is a need to understand the role of ozone and atmospheric optical absorption on the calibration of solar cells in the stratosphere.

REFERENCE

1. James R. Woodyard, “Laboratory Instrumentation and Techniques for Characterizing Multi-Junction Solar Cells,”Proceedings of the Twenty-Fifth Photovoltaic Specialists Conference, page 203, 1996.

2. Geoffrey A. Landis and Shelia G. Bailey, “Photovoltaic Engineering Testbed on International Space Station,” Proceedings of the Second World Conference on Photovoltaic Solar Energy Conversion, page 3564, 1998.

3. John A. Zoutendyk, “A Method for Predicting the Efficiency of Solar Cell Power Systems Outside the Earth’s Atmosphere,” NASA Technical Report No. 32-259 (1962).

4. Moon, P., “Proposed Standard Solar Radiation Curves for Engineering Use,” 1940, J. Franklin inst., 230, 583-617, 1940.

5. National Technical Information Office, ”Standard Atmosphere Model,” Springfield, Virginia (Product Number: ADA-035-6000).

6. Johnson, F. S., “The solar constant,” 1954, Journal of Meteorology, 11, 431-439.

7. D. W. Ritchie, “Development of Photovoltaic Standards for NASA,” Proceedings of the Fourth Photovoltaic Specialists Conference, page C-5-1, 1964.

8. Henry W. Brandhorst, Jr., “Airplane Testing of Solar Cells,” Proceedings of the Fourth Photovoltaic Specialists Conference, page C-2-1, 1964.

9. Henry W. Brandhorst, Jr., and Earle O. Boyer, “Calibration of Solar Cells Using High-Altitude Aircraft,” NASA Technical Note, NASA TN D-2508, February 1665.

10. E. Vigroux, “Contribution to the Experimental Study of the Absorption of Ozone,” Annales de Phys., vol. 8, page 709, 1953.

11. L. A. Biryukova, “Distribution of Energy in the Spectrum of Solar Rays a Various Altitudes,” JPRS 7488, Joint Pub. Res. Service, 1959. C. P. Hadley, Proceedings of the Fourth Photovoltaic Specialists Conference, page C-3-1, 1964.

12. C. P. Hadley, “Comparison of Flight and Terrestrial Solar Measurements on Silicon Cells,” Proceedings of the Fourth Photovoltaic Specialists Conference, page C-3-1, 1964.

13. Henry W. Brandhorst, Jr.,” Calibration of Solar Cells Using High-Altitude Aircraft,” Proceedings of the Fifth Photovoltaic Specialists Conference, page E-1-1, 1965.

14. Henry W. Brandhorst, Jr., “Anomalies in Solar Cell Langley Plots Associated with the Tropopause,” Applied Optics, vol. 7, page 716, 1968.

15. Philip Jenkins, David Brinker, and David Scheiman, “Uncertainty Analysis of High Altitude Aircraft Air Mass Zero Solar Cell Calibration,” Proceedings of the 26th Photovoltaic Specialists Conference, page 857, 1997.

16. David J. Brinker, David A. Scheiman, and Phillip Jenkins, “Calibration of Space Solar Cells Using High Altitude Aircraft,” Proceedings of the 2nd World Conference on Photovoltaic Solar Energy Conversion, page 3654, 1998.

17. http://powerweb.grc.nasa.gov/pvsee/facilities/scel/lear

18. David B. Snyder, David A. Scheiman, Philip P. Jenkins, William J. Rieke and Kurt S. Blankenship, “Ozone Correction for AM0 Calibrated Solar Cells for the Aircraft Method,” Proceedings of the 29th Photovoltaic Specialists Conference, page 832, 2002.

19. http://rredc.nrel.gov/solar/spectra/am0/NewAM0.xls

20. B. Leckner, “The Spectral Distribution of Solar Radiation at the Earth’s Surface – Elements of a Model,” Solar Energy, volume 20, page 143, 1978.

21. David B. Snyder, Philip P. Jenkins and David A. Scheiman, “Historical Precision of an Ozone Correction Procedure for AM0 Solar Cell Calibration,” Proceedings of the Space Photovoltaic Research and Technology Conference, 2003, In Press.

22. Richard D. McPeters, P. K. Bahartia, Arlin J. Krueger, Jay R. Herman, Charles G. Wellemeyer, Colin J. Seftor, Glen Jaross, William Byerly, Steven L. Taylor, Tom Swissler and Richard P. Cebula, “Earth Probe Total Ozone Mapping Spectrometer (TOMS) Data Products User’s Guide,” NASA Technical Publication 1998-206895, page 53, 1998.

23. IBID, page 53.

24. John A. Zoutendyk, “The Space Calibration of Standard Solar Cells Using High Altitude Balloon Flights,” Proceedings of the Fourth Photovoltaic Specialists Conference, page C-4-1, 1964.

25. B. E. Anspaugh and R. L. Mueller, ”Results of the 2002 JPL Balloon Flight Solar Cell Calibration Program,” JPL Publication 02-03, 2002.

26. IBID, page 20.

27. IBID, page 22.

28. IBID, page 26.

29. IBID, page 1.

30. Glenroy A. Bowe, Qianghua Wang, James R. Woodyard, Richard R. Johnston and William J. Brown, “Investigations to Characterize Multi-Junction Solar Cells in the Stratosphere Using Low-Cost Balloon and Communication Technologies,” Proceedings of 16th NASA Space Photovoltaic Research and Technology Conference, August 31-Septermber 2, 1999, page 189.

31. Glenroy A. Bowe, Qianghua Wang and James R. Woodyard, ”Investigations to Characterize Multi-junction Solar Cells in the Stratosphere Using Low-Cost Balloon and Communication Technologies,” Twenty-Eight IEEE Photovoltaic Specialists Conference Proceedings, 2000, page 1328.

32. Ali Mirza, David Sant, James R. Woodyard, Richard R. Johnston and William J. Brown, “Report on Project to Characterize Multi-junction Solar Cells in the Stratosphere Using Low-Cost Balloon and Communication Technologies,” Seventeen Space Photovoltaic Research and Technology Conference, 2001, page 137.